Molecular and Cellular Neuroscience 76 (2016) 68–75

Contents lists available at ScienceDirect

Molecular and Cellular Neuroscience

journal homepage: www.elsevier.com/locate/ymcne

Mitochondrial dynamics following global cerebral ischemia

Rita Kumar Ph.D. [a,b,c], Melissa J. Bukowski M.S. [a,b,c], Joseph M. Wider B.S. [b,c], Christian A. Reynolds Ph.D. [a,b,c], Lesley Calo M.S. [a,b,c], Bradley Lepore B.S. [a,b], Renee Tousignant M.Sc. [a,b], Michelle Jones M.S. [a,b], Karin Przyklenk Ph.D. [a,b,c], Thomas H. Sanderson Ph.D. [a,b,*]

[a] Department of Emergency Medicine, Wayne State University School of Medicine, Detroit, MI 48201, United States
[b] Cardiovascular Research Institute, Wayne State University School of Medicine, Detroit, MI 48201, United States
[c] Department of Physiology, Wayne State University School of Medicine, Detroit, MI 48201, United States

ARTICLE INFO

Article history:
Received 20 November 2015
Revised 19 August 2016
Accepted 24 August 2016
Available online 25 August 2016

Keywords:
Brain ischemia
Reperfusion
Mitochondrial dynamics
Opa1

ABSTRACT

Global brain ischemia/reperfusion induces neuronal damage in vulnerable brain regions, leading to mitochondrial dysfunction and subsequent neuronal death. Induction of neuronal death is mediated by release of cytochrome *c* (cyt *c*) from the mitochondria though a well-characterized increase in outer mitochondrial membrane permeability. However, for cyt *c* to be released it is first necessary for cyt *c* to be liberated from the cristae junctions which are gated by Opa1 oligomers. Opa1 has two known functions: maintenance of the cristae junction and mitochondrial fusion. These roles suggest that Opa1 could play a central role in both controlling cyt *c* release and mitochondrial fusion/fission processes during ischemia/reperfusion. To investigate this concept, we first utilized *in vitro* real-time imaging to visualize dynamic changes in mitochondria. Oxygen-glucose deprivation (OGD) of neurons grown in culture induced a dual-phase mitochondrial fragmentation profile: (i) fragmentation during OGD with no apoptosis activation, followed by fusion of mitochondrial networks after reoxygenation and a (ii) subsequent extensive fragmentation and apoptosis activation that preceded cell death. We next evaluated changes in mitochondrial dynamic state during reperfusion in a rat model of global brain ischemia. Evaluation of mitochondrial morphology with confocal and electron microscopy revealed a similar induction of fragmentation following global brain ischemia. Mitochondrial fragmentation aligned temporally with specific apoptotic events, including cyt *c* release, caspase 3/7 activation, and interestingly, release of the fusion protein Opa1. Moreover, we uncovered evidence of loss of Opa1 complexes during the progression of reperfusion, and electron microscopy micrographs revealed a loss of cristae architecture following global brain ischemia. These data provide novel evidence implicating a temporal connection between Opa1 alterations and dysfunctional mitochondrial dynamics following global brain ischemia.

1. Introduction

Patients who are successfully resuscitated following cardiac arrest often suffer serious neurologic complications that limit survival and/or functional recovery. The cerebral consequences of transient global ischemia are often quite severe and selectively damage vulnerable brain regions, including the pyramidal neurons of the CA1 hippocampus. The specific molecular mechanisms by which CA1 neurons die are not completely understood, however it is well-established that mitochondria play a central role in cell demise (Sims & Pulsinelli, 1987; Fiskum et al., 2004; Niizuma et al., 2010).

Release of cyt *c* from the intermembranous space of the mitochondria is a critical step in apoptosis induction and is generally thought to be controlled by increased permeability of the outer mitochondrial membrane to allow cyt *c* to cross into the cytosol. Release of cyt *c*, however, is a highly regulated process that requires more than outer membrane permeabilization (Yamaguchi et al., 2008). Under normal conditions, over 85% of cyt *c* is confined within the cristae folds of the inner mitochondrial membrane by protein complexes that maintain cristae junctions.

The cristae junctions are composed of complex oligomers of short and long isoforms of Opa1 and the balance of these isoforms dictates the structure or "tightness" of the cristae junction (Arnoult et al., 2005a; Frezza et al., 2006). Disruption of cristae junctions (*i.e.* Opa1 complexes) has been shown to be triggered by intrinsic apoptosis activation and is central for cyt *c* release independent of outer membrane permeabilization (Arnoult et al., 2005a; Frezza et al., 2006; Olichon et al., 2003). We have previously shown that in neurons Opa1 is released into the cytosol following both oxidative injury and OGD/reoxygenation *in vitro* (Sanderson et al., 2015a; Sanderson et al., 2015b). In these studies, proteolytic processing of Opa1, Opa1 oligomeric breakdown, and

* Corresponding author at: Department of Emergency Medicine, Wayne State University School of Medicine, Detroit, MI 48201, United States.
E-mail address: tsanders@med.wayne.edu (T.H. Sanderson).

http://dx.doi.org/10.1016/j.mcn.2016.08.010

Opa1 release was observed with cyt *c* release. Evidence of a central role for Opa1 regulation in cerebral injury has also been shown in models of focal ischemic insults to the neonate (Baburamani et al., 2015) and adult brain (Varanita et al., 2015).

In addition to the role of Opa1 in maintenance of the cristae junction, it is also well-established that Opa1 is an indispensable component of the mitochondrial fusion machinery. Proteolytic processing and altered expression of Opa1 isoforms have been shown to play key roles in mitochondrial fusion, with disruptions in Opa1 isoforms promoting a mitochondrial fission phenotype (Yamaguchi et al., 2008; Ehses et al., 2009). Evidence supporting a post-ischemic increase in mitochondrial fragmentation was provided by mitochondrial-YFP reporter mice exposed to brain ischemia (Owens et al., 2015). Indeed, mitochondrial fragmentation was observed following ischemia in the regions surrounding the CA1 pyramidal neurons in the striatum radiatum and striatum oriens of the CA1. However, due to imaging limitations, mitochondrial dynamics in the pyramidal neuron cell bodies of the CA1 were not reported. These data from our group and others lead us to hypothesize that Opa1 could be playing a central role in regulating cell death after global brain ischemia, and could be involved in post-ischemic mitochondrial fragmentation. Here, we proposed that the release of cyt *c* following global brain ischemia would be associated with disruption of Opa1 oligomers, thereby disrupting the balance of fusion and fission to promote mitochondrial fission and cell death.

2. Methods

2.1. Cell culture

HT22 murine hippocampal neurons were used for all *in vitro* experiments and were kindly provided by Dr. David Schubert (The Salk Institute, La Jolla, *CA*). Cells were transfected with mito-GFP plasmids (mitochondria-GFP: AcGFP1-Mito 632432, ClonTech) for 24 h utilizing opti-MEM media and 239fectin transfection reagent (Invitrogen). Cells were plated on glass-bottom culture dishes and experiments were conducted in a microscope chamber (Zeiss/PeCon). Baseline measurements were taken under normoxic conditions and cells were subjected to 45 min of oxygen-glucose deprivation (OGD) by bubbling glucose-free media in a sealed flask with 95% N_2/5% CO_2, then perfusing the media through a sealed system into the culture dish, exchanging the normal media with ischemic media at a rate of 0.5 mL/min. Pericellular O_2 was further reduced by active gas exchange using gas-permeable tubing (Teflon AF2400) connected to a gas mixer. Importantly, control experiments confirmed that the gas exchange protocol did not cause bubbling of the media or mechanical disruption of the cells. After the 45 min OGD insult, a second controlled exchange was performed, restoring normoxic and high-glucose media to the cultures. To monitor cell death caused by apoptosis, the substrate-based caspase-3/7 assay Magic Red® (MR-$(DEVD)_2$) was added to media. MR-$(DEVD)_2$ fluoresces red (emission at 610 nm) when it is cleaved by active caspase-

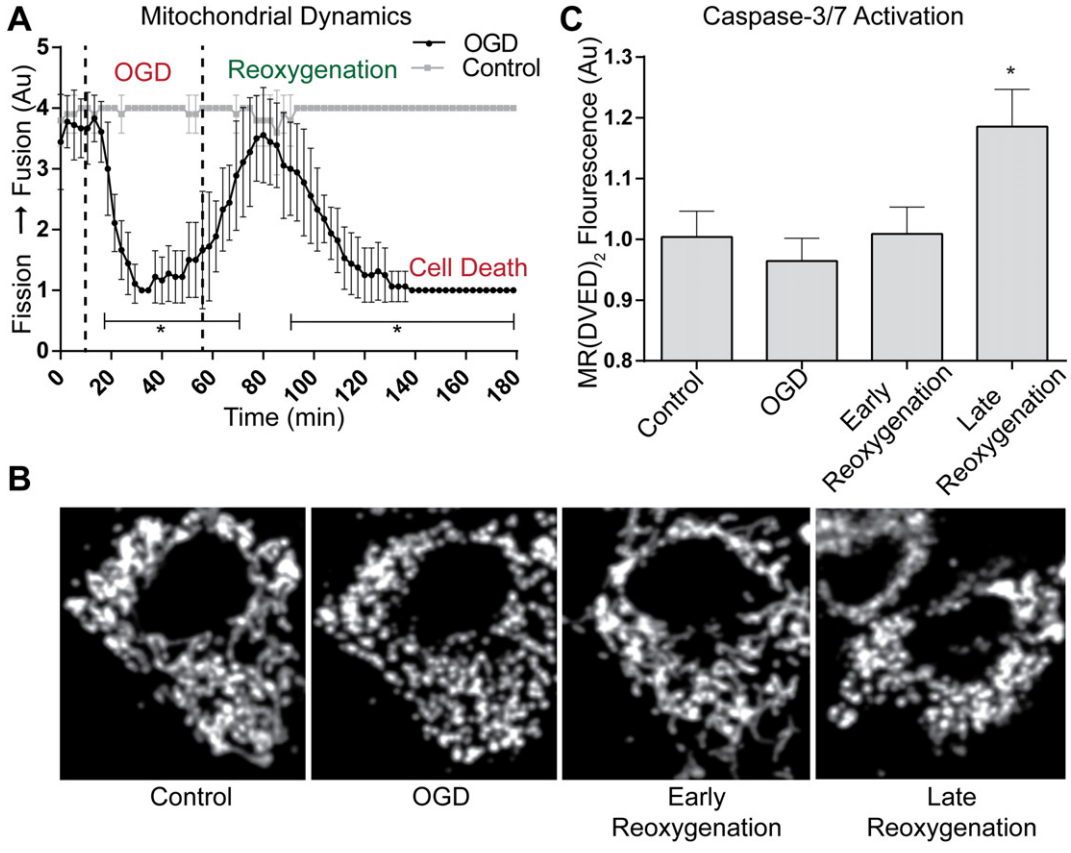

Fig. 1. Mitochondrial dynamics and caspase-3/7 activation during OGD and reoxygenation. (A) Graphical representation of fission/fusion index (Supplementary Fig. 1) during the progression of OGD/Reoxygenation (Mean ± SD). (A & B) Baseline measurements of mitochondrial morphology include both small, fragmented and long, tubular mitochondrial. During OGD induction, rapid fragmentation occurs. Upon reoxygenation mitochondrial morphology returns to a control state (Early Reoxygenation). As reoxygenation is prolonged, mitochondria undergo rapid and irreversible fragmentation, coinciding with cell death (Late Reoxygenation) [n = 18 significant differences in control *vs.* OGD shown in brackets ($p < 0.05$)]. (C) Caspase activation was measured at designated stages of the experiment. During late reoxygenation (60 min after reoxygenation), MR-$(DVED)_2$ fluorescence was significantly increased *versus* control (*$p < 0.05$).

3/7. Cells were visualized at 40× for mito-GFP and for MR-$(DEVD)_2$ activation. Exposures were taken every 30 s for the duration of the experiment (approximately 5 h). The z-stacks were set with images collected per 1 μm optical section. Volocity software (Perkin Elmer) was used for image acquisition. Images were evaluated as z-projections for changes in mitochondrial morphology. Mitochondrial morphology was qualitatively assessed by applying a scoring system ranging from 1 to 5. A score of 1 denoted completely punctate or fragmented mitochondria (>90% fragmented), while a score of 5 represented mitochondria that are fully fused into a webbed network or long interconnected mitochondria. Intermediate fission/fusion states were given scores ranging from 2 to 4 depending on the balance of these phenotypes, as depicted in Supplementary Fig. 1. Cells in multiple regions of interest were randomly selected to be analyzed and scored, frame-by-frame over the entirety of each experiment.

2.2. Animal model

Animal experiments in this study were approved by the Wayne State University Institutional Animal Care and Use Committee and conform to the guidelines presented in the National Research Council's *Guide for the Care and Use of Laboratory Animals*, 8th Edition. Global brain ischemia of 8-min duration was induced using bilateral carotid occlusion and hypotension as originally described by Smith et al. (1984) with modifications by Sanderson et al. (2008) and Sanderson & Wider (2013). Male Sprague-Dawley rats weighing 325 to 375 g were anesthetized with isofluorane, orotracheally intubated, and mechanically ventilated. Rectal temperature was maintained at 37.0 ± 0.5 °C. The femoral artery was accessed with a PE-50 catheter and invasive blood pressure monitored (PowerLab, AD Instruments). Cerebral blood flow was recorded using a laser Doppler flow probe (AD Instruments). Ischemia was induced by first rapidly withdrawing (within 1 min) 8–10 CCs of blood from the femoral arterial catheter to achieve a target mean arterial pressure of 30 ± 1 mm Hg. Both common carotid arteries were then transiently occluded with microaneurysm clips. After 8 min of global brain ischemia, the clips were removed and blood slowly restored through the femoral artery (2 CCs per minute). Sham-operated control animals were subjected to surgery but no ischemia and kept under anesthesia for equal durations and doses.

2.3. Subcellular fractionation

Following defined durations of reperfusion, animals were transcardially perfused with ice-cold normal saline and the brain was removed. The hippocampi were microdissected and homogenized with 15 strokes of a Potter-Elvehjem tissue homogenizer (pestle 0.2 mm clearance, 150 rpm, 4 °C) in 1:5 (wt:vol) mitochondrial isolation media (20 mM HEPES, 250 mM sucrose, 10 mM KCl, 1.5 mM MgCl2,

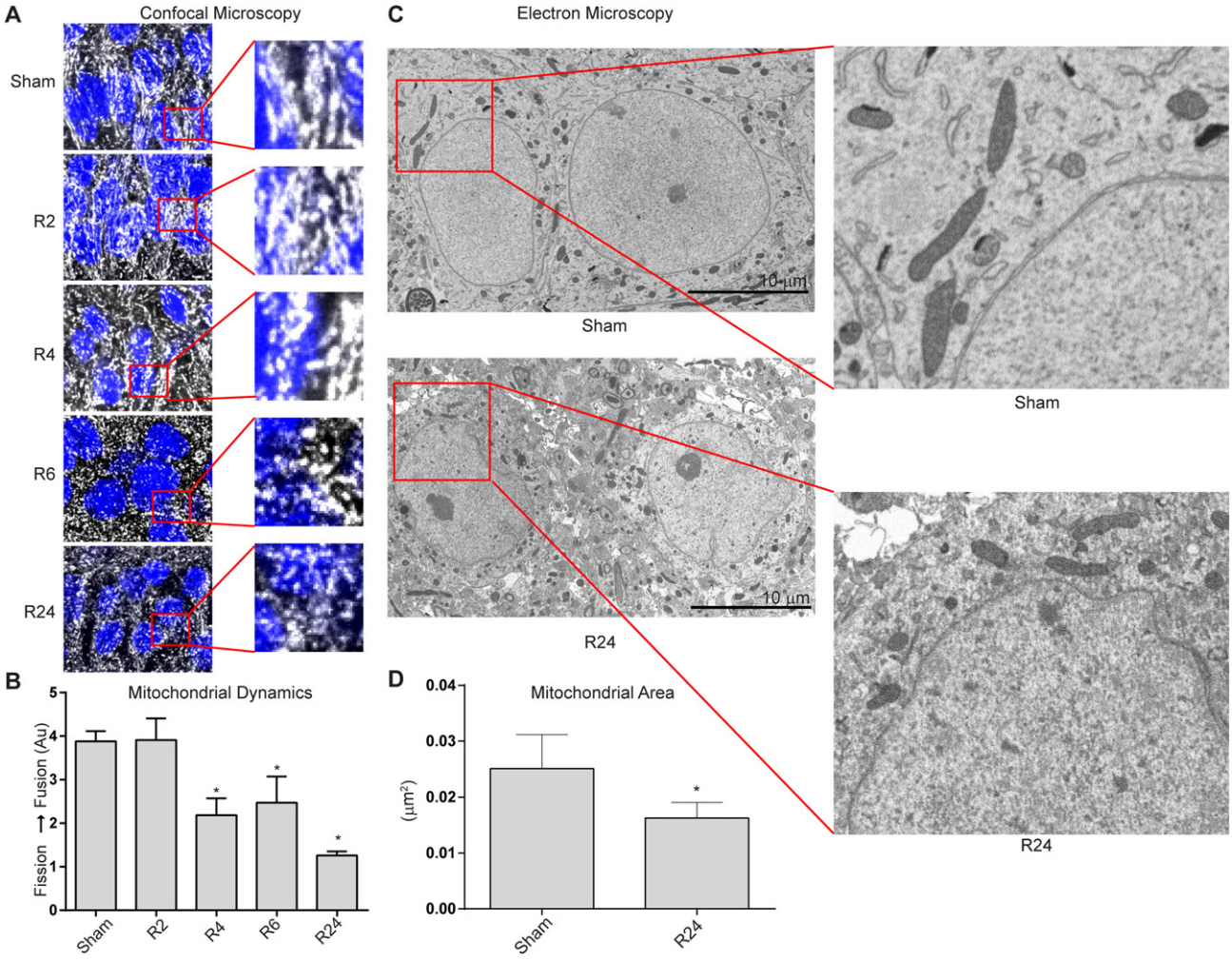

Fig. 2. Mitochondrial dynamics following global brain ischemia. (A) Morphologic changes in mitochondria were assessed using ATP synthase immunofluorescence (grayscale) while cell nuclei were identified with DAPI (blue). Significant mitochondrial fragmentation is evident after 4, 6, and 24 h of reperfusion following global brain ischemia (R4, R6, and R24) compared to sham-operated controls and after 2 h of reperfusion (Sham, R2; *$p < 0.05$, n = 5/group). (B) Graphical representation of fission/fusion index (Supplementary Fig. 1) following global brain ischemia (Mean ± SD). (C) Electron microscopy images of CA1 hippocampal neurons in controls (Sham) and after 24 h of reperfusion (R24). (D) Graphical representation of the mitochondrial area (Mean ± SD; *$p < 0.05$, n = 3/group).

1 mM EGTA, 1 mM EDTA) supplemented with protease inhibitors (0.2 mM PMSF, 1 μg/mL pepstatin, 10 μg/mL aprotinin, 10 μg/mL leupeptin), and then centrifuged at 750 ×*g* for 10 min. The resulting supernatant was centrifuged at 13,500 ×*g* for 10 min, and the pellet taken as the crude mitochondrial fraction. The remaining supernatant was centrifuged at 100,000 ×*g* for 60 min and the supernatant was taken as the cytosolic fraction. All fractions were immunoblotted for housekeeping proteins for cytosol and mitochondria to verify purity of the isolations. This preparation results in a cytosolic fraction with no detectable cytochrome *c* oxidase subunit IV as previously described (Sanderson et al., 2008).

2.4. Blue native-PAGE

Mitochondrial fractions were lysed in 1:5 (wt:vol) lysis buffer containing protease and phosphatase inhibitors (0.5% Nonidet P-40, 10 mM Tris-HCl pH 7.4, 142.5 mM KCl, 5 mM $MgCl_2$, 1 mM EGTA, 10 μg/mL aprotinin, 1 μg/mL leupeptin, 1 μg/mL pepstatin, 0.1 mM phenylmethylsulphonylfluoride). Enriched mitochondrial lysates were diluted to a concentration of 1 μg/μL and incubated in 0.5% n-dodecyl β-D-maltoside (DDM) for 20 min before being loaded into custom-made native 5–12% gradient gels and run at 240 V at 4 °C as previously described (Wittig et al., 2006).

2.5. Western blotting

Equal amounts of protein (20–50 μg depending on the fraction) were resolved using SDS-PAGE or BN-PAGE and then transferred to nitrocellulose. Membranes were incubated in primary antibody (1:500 to 1:1000, according to manufacturer's specifications) followed by secondary antibody (1:10,000 dilution). Primary antibodies used for immunoblotting were cytochrome *c* (BD Biosciences), COX subunit IV (Invitrogen), or ATP synthase (Chemicon), and Opa1 (Novus). Antibody binding was detected using the enhanced chemiluminescence technique (GE Healthcare). Exposure times were adjusted to ensure that all band densities were within the linear range of the film. Blots were analyzed using scanning densitometry and Image Studio software (LI-COR) and were normalized to the corresponding loading control.

2.6. Transmission electron microscopy

Brains were perfusion-fixed with 2.5% gluteraldehyde and microdissected to isolate the CA1 hippocampal region. Tissue blocks were counterstained with 1% osmium tetroxide, dehydrated, and embedded in Durcupan resin. Ultrathin (70 nm) sections were taken with a diamond blade, counterstained with lead citrate, and imaged on a JOEL 2010

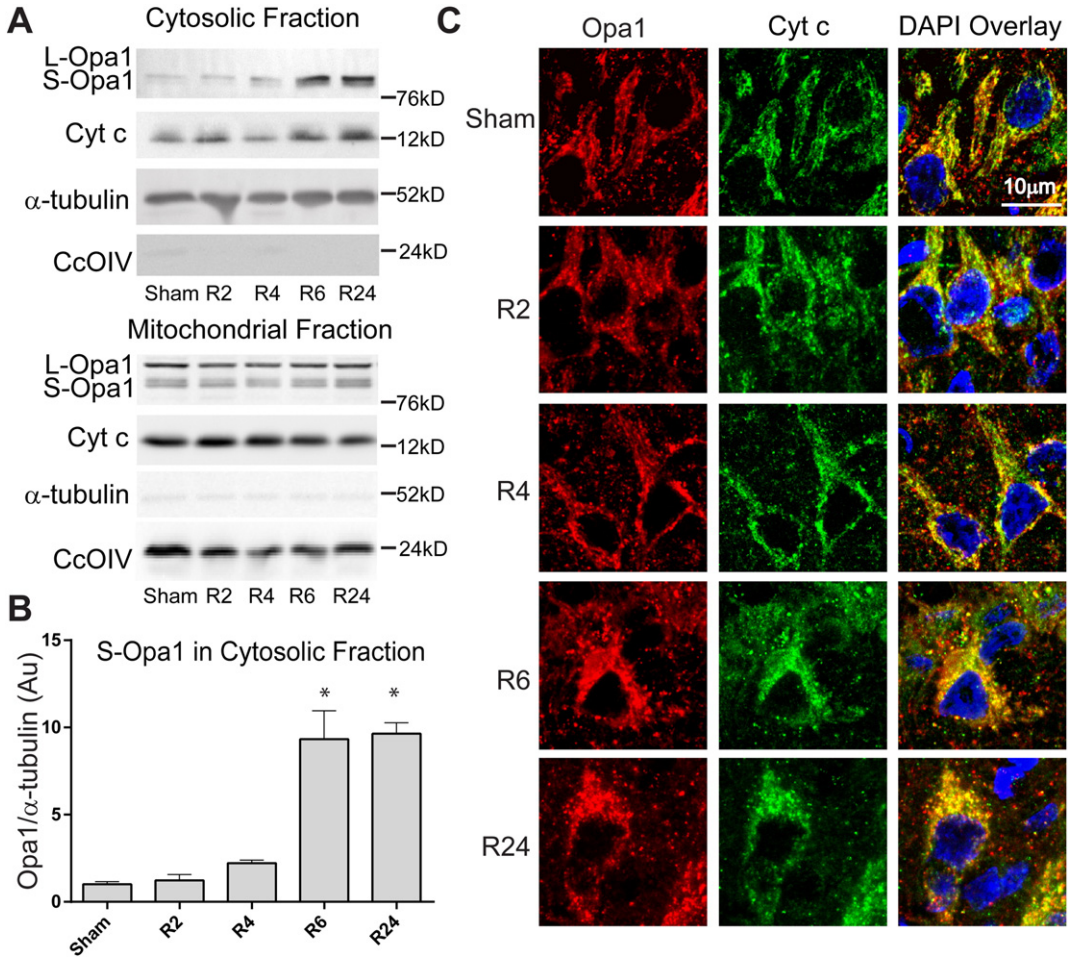

Fig. 3. Opa1 and cytochrome *c* release following global brain ischemia. Opa1 and cyt *c* immunoreactivity were assayed by (A & B) Western blot of subcellular fractions of CA1 and (C) immunofluorescence in tissue slices. Sham-operated rats had little immunoreactivity of Opa1 and cyt *c* in cytosolic fractions and punctate Opa1 and cyt *c* staining in neurons of the CA1, consistent with mitochondrial localization. Ischemia followed by 6 or 24 h of reperfusion show increases in cytosolic Opa1 and cyt *c* and diffuse immunofluorescence in the CA1, consistent with Opa1 and cyt *c* release.

transmission electron microscope. Random images (9 per animal) were selected for mitochondrial area quantification. Mitochondria in 3 cells per image were traced in ImageJ and the average mitochondrial area in the 21 cells was depicted as the average mitochondrial area.

2.7. Immunofluorescence

Rats were transcardially perfused with 4% paraformaldehyde, post-fixed, cryoprotected in 30% sucrose in PBS, and then snap frozen for cryosectioning. The hippocampus was serially sectioned on a cryostat between 2.1 mm and 3.3 mm posterior to bregma at a thickness of 20 μm as we previously described (Sanderson et al., 2008; Sanderson & Wider, 2013). Sections were quenched in 3% hydrogen peroxide, then incubated in blocking solution (5% normal goat serum and 0.3% Triton X-100 in Tris-buffered saline). Next, the sections were incubated with primary antibodies (COX subunit IV, 1:50, Cell Signaling; ATP synthase, 1:100, Chemicon; Opa, 1:100, Cell Signaling; or cytochrome *c*, 1:100, Abcam). Sections were incubated with AlexaFluor-conjugated secondary antibodies (1:100, Life Sciences), then mounted and cover slipped. Slides were imaged on a Leica SP5 confocal microscope at a z-plane interval of 0.25 μm. Eight sequential optical sections were flattened into a z-projection for analysis.

2.8. Statistics

Data were graphed using GraphPad Prism 6, and data from control *vs.* OGD exposed cells over time were statistically evaluated for differences using two-way ANOVA for multiple comparisons at $p < 0.05$, followed by *post hoc* analysis for differences at individual time points with Sidak's multiple comparisons test. All other data were compared with one-way ANOVA followed by Tukey's test for *post hoc* evaluation of significant differences at $p < 0.05$.

3. Results

3.1. Mitochondrial dynamics during oxygen-glucose deprivation/reoxygenation

Our previous studies utilized static endpoints in isolated cell systems to evaluate mitochondrial changes following OGD and oxidative injury (Sanderson et al., 2015c; Sanderson et al., 2015b). Here we sought to evaluate the temporal progression of mitochondrial dynamics *in vitro*. We induced OGD followed by reoxygenation continually imaging neurons with a confocal microscope. Alterations in mitochondrial morphology were assessed utilizing a 1–5 scale to characterize changes in organelle networks (Supplementary Fig. 1). Thorough visual analysis of all time-lapse images was utilized to identify the dynamic state of mitochondria throughout the cell. This methodology allows clear evaluation of the entire z-stack, especially in the perinuclear region where accumulation of small-fragmented mitochondria can be misidentified as long mitochondria due to limited z-plane resolution. The baseline mitochondrial dynamic state showed a steady balance (scored 3) to moderately-fused network (scored 4), signifying a stable homeostatic state (Fig. 1A-Tabulated Data; Fig. 2B and Supplementary Fig. 2-Timelapse images). Upon initiation of OGD, mitochondria rapidly underwent fission, with all cells transitioning to a phenotype of mitochondrial fission (average score = 1, $^*p < 0.05$ *versus* control). Mitochondria reorganize into a networked mitochondrial morphology after reoxygenation and collectively regain the control state. This interconnected and balanced state was transient, as a second fragmentation event ensued during late reoxygenation ($^*p < 0.05$ *versus* control). In contrast with the mitochondrial fragmentation observed during ischemia, this reoxygenation-induced fragmentation did not recover to control state and culminated in caspase-3/7 activation as detected with Magic Red© ($MR\text{-}DEVED_2$-Fig. 1C). Control cells showed no change in the baseline mitochondrial

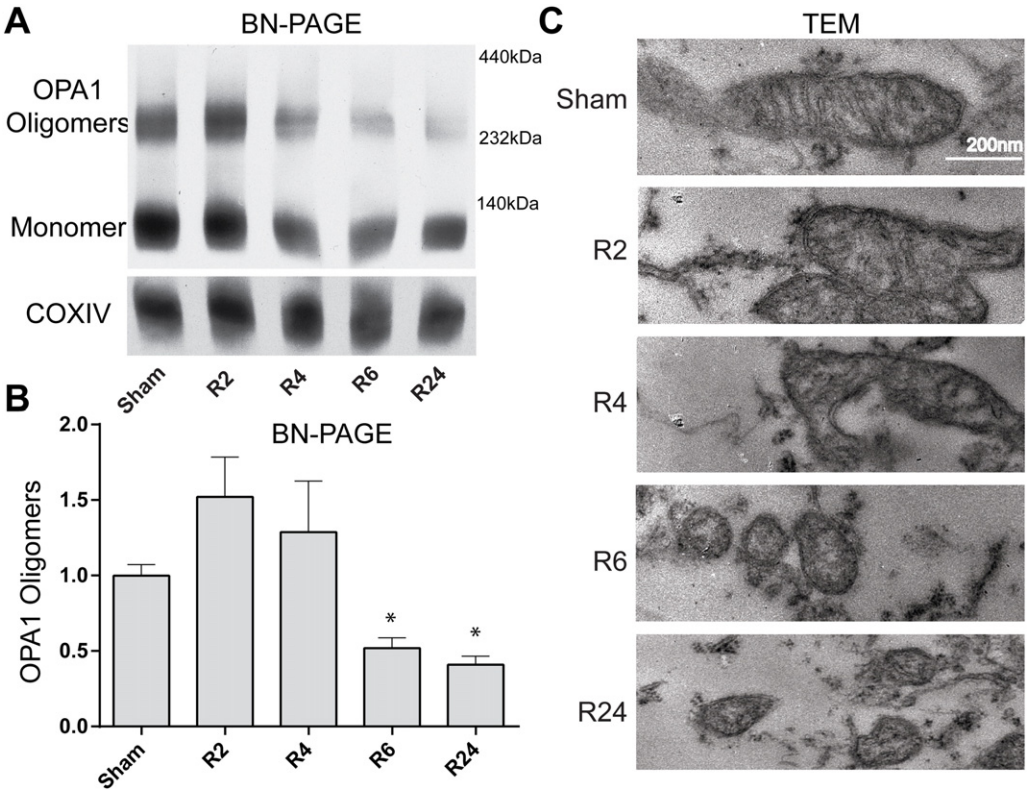

Fig. 4. Opa1 oligomer and mitochondrial cristae integrity. (A & B) BN-PAGE of mitochondrial samples demonstrated Opa1 exists in both monomeric and oligomeric state in sham-operated animals. Following ischemia and 6 h of reperfusion (R6) there is a significant decrease in Opa1 oligomers that remains decreased at 24 h following ischemia (R24). (C) Cristae morphology was analyzed by transmission electron microscopy. Sham brains showed ordered cristae with an elongated mitochondrial morphology. At 6 and 24 h of reperfusion, mitochondria are small and fragmented with a loss of normal cristae structure.

dynamic state or caspase-3/7 activation with 5 h of equivalent rate perfusion and image acquisition.

3.2. Mitochondrial fragmentation after global brain ischemia

Utilizing these cell culture findings as a guide, we next sought to determine the mitochondrial dynamic state in neurons during reperfusion in an animal model of global brain ischemia. *In vitro*, we found a dual phase fragmentation profile, where ischemia resulted in a reversible fragmentation phase that was not associated with caspase-3/7 activation and a secondary reperfusion-induced fragmentation phase where caspase-3/7 was activated followed by cell rupture. We focused our evaluation of the dynamic state of mitochondria on early and late stages of reperfusion based on the time course of cell death established in our previous studies (Sanderson et al., 2008; Sanderson et al., 2013). Mitochondria were labeled with antibodies specific for mitochondrial proteins: ATP synthase (Fig. 2) or cytochrome *c* oxidase subunit IV (Supplementary Fig. 3). Images were assigned numerical scores based on criteria described for *in vitro* experiments (Supplementary Fig. 1). Confocal microscopy of neurons following global brain ischemia revealed marked alterations in mitochondrial morphology. In sham-operated control animals, mitochondria were in long, tubular networks with some punctate, fragmented mitochondria; a state similar to that observed at baseline *in vitro*. Following 4 h of reperfusion the intracellular mitochondrial network score shows a significant reduction in filamentous mitochondria and increased mitochondrial fragmentation (Fig. 2, $^{*}p < 0.05$). Mitochondrial fragmentation phenotype progresses and is distinct at 6 and 24 h of reperfusion ($^{*}p < 0.05$).

We then further validated and quantified the change in mitochondrial size, using randomly selected transmission electron microscopy images from rats exposed to global brain ischemia and 24 h of reperfusion compared to sham-operated control animals. In congruence with our immunofluorescence studies, the mean mitochondrial area was reduced by 64% following 24 h of reperfusion (Fig. 3C & D; $^{*}p < 0.05$).

3.3. Opa1 release from the mitochondria

Mitochondrial fragmentation has been linked with execution of apoptosis and cell death in multiple studies (Sanderson et al., 2015b; Sanderson et al., 2015a; Brooks et al., 2011; Karbowski & Youle, 2003; Wasiak et al., 2007). Alterations in the proportion of Opa1 isoforms and release of Opa1 into the cytosol have been implicated in cristae remodeling leading to cyt *c* release and induction of mitochondrial fission (Arnoult et al., 2005a; Varanita et al., 2015; Frezza et al., 2006; Sanderson et al., 2015b; Sanderson et al., 2015a). Here we assayed Opa1 and cyt *c* release by both Western blotting subcellular fractions of CA1 hippocampus and immunofluorescence in tissue sections (Fig. 3). Opa1 is present in both long and short isoforms in the mitochondrial fraction of CA1 neurons in Sham-operated animals. There is no significant increase in cytosolic Opa1 at 2 and 4 h of reperfusion (R2 and R4,

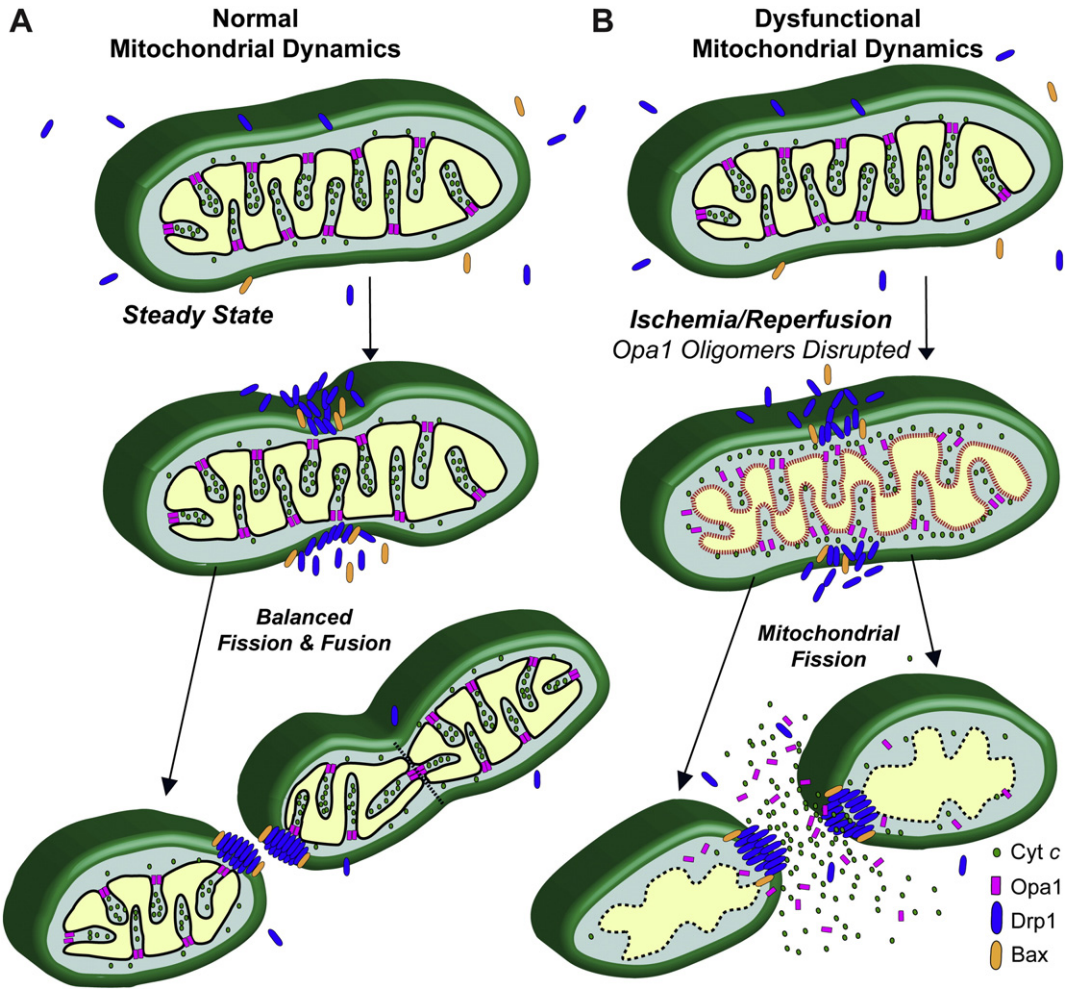

Fig. 5. Proposed mechanism of Opa1-mediated mitochondrial fragmentation. (A) Normal steady-state mitochondrial dynamics with balanced mitochondrial fission and fusion. (B) Proposed disruption of mitochondrial dynamics following brain ischemia. Opa1 oligomer disruption leads to both liberation of cyt *c* from the cristae folds and attenuation of mitochondrial fusion. Mitochondrial fission is associated with outer mitochondrial membrane permeablization. These events culminate in a fragmented phenotype and cyt *c* and Opa1 release into the cytosol. Figure adapted from (Calo et al., 2013).

respectively). Short isoforms of Opa1 are significantly increased in the cytosol after 6 h of reperfusion in the CA1 hippocampal region (Fig. 3). Cytosolic Opa1 remains significantly increased at 24 h of reperfusion (*$p < 0.05$). Opa1 isoforms (short and long) were not significantly changed at any time point analyzed following ischemia. Mitochondrial release of Opa1 coincides with cyt *c* release and is consistent with the time course of fragmentation (Fig. 2). Immunofluorescence of Opa1 and cyt *c* show punctate staining in sham-operated controls, indicative of mitochondrial co-localization. Following ischemia, Opa1 and cyt *c* immunoreactivity changes from a punctate-mitochondrial localization to a diffuse cytosolic distribution by 6 and 24 h of reperfusion. This localization change demonstrating release of both Opa1 and cyt *c* during reperfusion is consistent with Western blot of mitochondrial and cytosolic fractions (Fig. 3).

3.4. Mitochondrial Opa1 complex breakdown following brain ischemia

Release of Opa1 into the cytosol (Fig. 3) and mitochondrial fragmentation (Figs. 1 and 2) are key events associated with loss of cristae junction integrity and subsequent apoptosis (Arnoult et al., 2005a). To determine if the cristae junction structure was indeed altered, we assayed Opa1 oligomeric complex formation utilizing BN-PAGE of mitochondrial samples from brains exposed to global brain ischemia. BN-PAGE of mitochondrial fractions showed loss of high-molecular weight Opa1 oligomers at 6 and 24 h of reperfusion in CA1 hippocampus (Fig. 4A and B, *$p < 0.05$).

3.5. Loss of cristae morphology and increased fragmented mitochondria following brain ischemia

To further examine changes at the ultrastructural level, we assessed mitochondrial ultrastructure in CA1 hippocampal neurons by electron microscopy (Fig. 4C). Supporting the confocal microscopy imaging results utilizing immunofluorescence of mitochondrial markers, the mitochondrial morphology in sham-operated control animals was tubular in TEM images. In contrast to control animals, the morphology of mitochondria was altered in post-ischemic brains with the appearance of morphologic constriction points in mitochondria at 2 and 4 h of reperfusion and small fragmented mitochondria at 6 and 24 h of reperfusion. Consistent with Opa1 oligomeric breakdown, TEM revealed a loss of organized cristae structure at 6 and 24 h of reperfusion (all groups $n = 4–6$). These data support the model that altered mitochondrial dynamics and loss of inner mitochondrial membrane integrity manifest during reperfusion injury.

4. Discussion

Integrity of cristae and the outer mitochondrial membrane play a pivotal role in determining neuronal cell fate in the setting of ischemia-reperfusion injury. Moreover, the pathophysiologic stress of ischemia-reperfusion will, in theory, 'prime' neurons for an up-regulation in fission (Sobrado et al., 2012; Aurora et al., 2012; Wang et al., 2011). There is morphologic evidence supporting mitochondrial fragmentation induction by ischemia-reperfusion, which is further strengthened with molecular data identifying interactions and interrelationships among key proteins involved in apoptosis, fission and fusion (Owens et al., 2015; Arnoult et al., 2005a; Frezza et al., 2006; Yamaguchi et al., 2008). There has been considerable research focused on the fission protein, Drp1, as the connection between mitochondrial fragmentation and cell death. For example, Drp1 reportedly co-localizes with members of the Bcl-2 family proteins (Bax and tBid) (Arnoult et al., 2005a) at the level of the mitochondria, and blocking this attenuates fission and enhances cell survival (Chen et al., 2005). More specifically, Bax has been shown to accumulate at fission points, possibly as a component of a functional unit including Drp1 and Mfn2, with both Bax and Mfn2 thus forming part of the fission complex (Wong et al., 2000; Makino et al., 2010; Brooks et al., 2011; Ljubicic et al., 2010). Furthermore, manipulation of mitochondrial dynamics by over-expressing a dominant-negative Drp1 demonstrated impaired mitochondrial fission in response to apoptotic stimuli and inhibition of both cyt *c* release and apoptotic cell death (Germain et al., 2005). Drp1 translocation presents a logical connection between mitochondrial fission and apoptosis. Despite these insights, however, it is not known whether fission is an active participant in the induction or execution apoptosis or conversely, whether fission is simply a bystander consequence of cell death.

While multiple studies have reported Drp1 translocation and increased mitochondrial fission in conjunction with apoptosis (Arnoult et al., 2005b; Estaquier & Arnoult, 2007; Ong et al., 2010), the contribution of Drp1-mediated fragmentation in the setting of cerebral ischemia/reperfusion is not clear. Early studies demonstrated a causal role for Drp1 mediated fission in apoptosis and cell death following *in vitro* ischemia and *in vivo* ischemic stroke (Grohm et al., 2012). More recent studies suggest a more nuanced role for Drp1-mediated fragmentation. While inhibition of Drp1 with mdivi1 reduced ischemic damage, it paradoxically increased injury during reperfusion (Zuo et al., 2014; Zhang et al., 2013). These studies suggest the deleterious effects of blocking mitochondrial fission are due to inhibition of mitophagy and thus preventing clearance of damaged or defective mitochondria.

These studies clearly demonstrate that manipulating mitochondrial dynamics as a therapeutic approach requires a better understanding of the roles these processes play in post-ischemic cell death. Here we present a novel hypothesized mechanism (Fig. 5), where increased fission could result from either dysfunctional fusion alone or in concert with induction of fission. Disruption of Opa1 oligomers during reperfusion may be a novel mechanism contributing to mitochondrial fragmentation and cell death during reperfusion.

Mitochondrial fusion is critical for embryonic development, as demonstrated by the fact that genetic manipulation of key fusion proteins to impair fusion (*e.g.* double knockout of Mfn1 and Mfn2) is embryonically lethal (Chen et al., 2005). However, the process of fusion (and in particular physiological Opa1 localization) is required for the maintenance of normal mitochondrial architecture and function, with loss or knockdown of Opa1 resulting in fragmented mitochondria, disorganization of cristae structure, and initiation of apoptosis (Arnoult et al., 2005a; Wong et al., 2000; Olichon et al., 2003). Appropriate subcellular localization of Opa1 (secured to the inner mitochondrial membrane) also appears significant: the presence of Opa1 isoforms in the cytosol has only been detected in pathological situations (Arnoult et al., 2005a; Makino et al., 2010; Ljubicic et al., 2010; Ju et al., 2008). Finally, a recent report demonstrates that controlled transgenic over-expression of Opa1 can "tighten" cristae junctions, limit cytochrome *c* release, and provide protection from ischemic brain damage following stroke (Varanita et al., 2015).

Opa1 complex integrity is a marker of mitochondrial cristae organization and susceptibility to apoptotic cell death. Indeed, Opa1 has been shown to be subject to proteolytic processing into short isoforms, released into the cytosol, and disrupted oligomeric integrity in a myriad of pathological contexts (Sanderson et al., 2015b; Sanderson et al., 2015a; Varanita et al., 2015; Ju et al., 2008; Kushnareva et al., 2013; Makino et al., 2010; Ljubicic et al., 2010). Importantly, the loss of Opa1 function through silencing, gene knock-out, and dominant-negative isoform expression results in an inhibition of fusion, subsequent upregulating of fission, and increased susceptibility to cell death induction. Opa1 oligomeric alteration has been shown to be required for complete release of cyt *c* due to its ability to limit cyt *c* availability within the cristae regions of the intermembranous space (Frezza et al., 2006; Yamaguchi et al., 2008). These key findings and the data presented here suggest a mechanism where Opa1 must undergo alterations for apoptosis to ensue, thus tipping the balance of mitochondrial dynamics toward fission by inhibiting fusion.

These studies suggest a potential mechanism of cell death where key mediators of the physiologic mitochondrial dynamics process become

maladapted and actively participate in apoptosis (Fig. 5). We put forth a proposed sequence of events where the alterations in the dynamic state of mitochondria are not a consequence of physiologic responses to ischemia, but rather pathologic alterations in fusion that drive the balance of mitochondrial dynamics toward a fission phenotype and actively participate in cell death. Future studies must further interrogate these events through gain-and-loss of function approaches to better understand the potential connection between mitochondrial dynamics, Opa1, and post-ischemic brain injury.

Supplementary data to this article can be found online at http://dx.doi.org/10.1016/j.mcn.2016.08.010.

Acknowledgements

The research described in this manuscript was supported by grant R01NS76715 and R01091242 from the National Institutes of Health (THS, RK).

References

Arnoult, D., Grodet, A., Lee, Y.J., Estaquier, J., Blackstone, C., 2005a. Release of OPA1 during apoptosis participates in the rapid and complete release of cytochrome *c* and subsequent mitochondrial fragmentation. J. Biol. Chem. 280 (42), 35742–35750. http://dx.doi.org/10.1074/jbc.M505970200.

Arnoult, D., Rismanchi, N., Grodet, A., Roberts, R.G., Seeburg, D.P., Estaquier, J., Sheng, M., Blackstone, C., 2005b. Bax/Bak-dependent release of DDP/TIMM8a promotes Drp1-mediated mitochondrial fission and mitoptosis during programmed cell death. Curr. Biol. 15 (23), 2112–2118. http://dx.doi.org/10.1016/j.cub.2005.10.041.

Aurora, A.B., Mahmoud, A.I., Luo, X., Johnson, B.A., van Rooij, E., Matsuzaki, S., Humphries, K.M., Hill, J.A., Bassel-Duby, R., Sadek, H.A., Olson, E.N., 2012. MicroRNA-214 protects the mouse heart from ischemic injury by controlling Ca(2)(+) overload and cell death. J. Clin. Invest. 122 (4), 1222–1232. http://dx.doi.org/10.1172/JCI59327.

Baburamani, A.A., Hurling, C., Stolp, H., Sobotka, K., Gressens, P., Hagberg, H., Thornton, C., 2015. Mitochondrial optic atrophy (OPA) 1 processing is altered in response to neonatal hypoxic-ischemic brain injury. Int. J. Mol. Sci. 16 (9), 22509–22526. http://dx.doi.org/10.3390/ijms160922509.

Brooks, C., Cho, S.G., Wang, C.Y., Yang, T., Dong, Z., 2011. Fragmented mitochondria are sensitized to Bax insertion and activation during apoptosis. Am. J. Phys. 300 (3), C447–C455. http://dx.doi.org/10.1152/ajpcell.00402.2010.

Calo, L., Dong, Y., Kumar, R., Przyklenk, K., Sanderson, T.H., 2013. Mitochondrial dynamics: an emerging paradigm in ischemia-reperfusion injury. Curr. Pharm. Des. 19 (39), 6848–6857.

Chen, H., Chomyn, A., Chan, D.C., 2005. Disruption of fusion results in mitochondrial heterogeneity and dysfunction. J. Biol. Chem. 280 (28), 26185–26192. http://dx.doi.org/10.1074/jbc.M503062200.

Ehses, S., Raschke, I., Mancuso, G., Bernacchia, A., Geimer, S., Tondera, D., Martinou, J.C., Westermann, B., Rugarli, E.I., Langer, T., 2009. Regulation of OPA1 processing and mitochondrial fusion by m-AAA protease isoenzymes and OMA1. J. Cell Biol. 187 (7), 1023–1036. http://dx.doi.org/10.1083/jcb.200906084.

Estaquier, J., Arnoult, D., 2007. Inhibiting Drp1-mediated mitochondrial fission selectively prevents the release of cytochrome *c* during apoptosis. Cell Death Differ. 14 (6), 1086–1094. http://dx.doi.org/10.1038/sj.cdd.4402107.

Fiskum, G., Rosenthal, R.E., Vereczki, V., Martin, E., Hoffman, G.E., Chinopoulos, C., Kowaltowski, A., 2004. Protection against ischemic brain injury by inhibition of mitochondrial oxidative stress. J. Bioenerg. Biomembr. 36 (4), 347–352.

Frezza, C., Cipolat, S., Martins de Brito, O., Micaroni, M., Beznoussenko, G.V., Rudka, T., Bartoli, D., Polishuck, R.S., Danial, N.N., De Strooper, B., Scorrano, L., 2006. OPA1 controls apoptotic cristae remodeling independently from mitochondrial fusion. Cell 126 (1), 177–189. http://dx.doi.org/10.1016/j.cell.2006.06.025.

Germain, M., Mathai, J.P., McBride, H.M., Shore, G.C., 2005. Endoplasmic reticulum BIK initiates DRP1-regulated remodelling of mitochondrial cristae during apoptosis. EMBO J. 24 (8), 1546–1556.

Grohm, J., Kim, S.W., Mamrak, U., Tobaben, S., Cassidy-Stone, A., Nunnari, J., Plesnila, N., Culmsee, C., 2012. Inhibition of Drp1 provides neuroprotection in vitro and in vivo. Cell Death Differ. 19 (9), 1446–1458. http://dx.doi.org/10.1038/cdd.2012.18.

Ju, W.K., Lindsey, J.D., Angert, M., Patel, A., Weinreb, R.N., 2008. Glutamate receptor activation triggers OPA1 release and induces apoptotic cell death in ischemic rat retina. Mol. Vis. 14, 2629–2638.

Karbowski, M., Youle, R.J., 2003. Dynamics of mitochondrial morphology in healthy cells and during apoptosis. Cell Death Differ. 10 (8), 870–880. http://dx.doi.org/10.1038/sj.cdd.4401260.

Kushnareva, Y.E., Gerencser, A.A., Bossy, B., Ju, W.K., White, A.D., Waggoner, J., Ellisman, M.H., Perkins, G., Bossy-Wetzel, E., 2013. Loss of OPA1 disturbs cellular calcium homeostasis and sensitizes for excitotoxicity. Cell Death Differ. 20 (2), 353–365http://www.nature.com/cdd/journal/v20/n2/suppinfo/cdd2012128s1.html.

Ljubicic, V., Menzies, K.J., Hood, D.A., 2010. Mitochondrial dysfunction is associated with a pro-apoptotic cellular environment in senescent cardiac muscle. Mech. Ageing Dev. 131 (2), 79–88. http://dx.doi.org/10.1016/j.mad.2009.12.004.

Makino, A., Scott, B.T., Dillmann, W.H., 2010. Mitochondrial fragmentation and superoxide anion production in coronary endothelial cells from a mouse model of type 1 diabetes. Diabetologia 53 (8), 1783–1794. http://dx.doi.org/10.1007/s00125-010-1770-4.

Niizuma, K., Yoshioka, H., Chen, H., Kim, G.S., Jung, J.E., Katsu, M., Okami, N., Chan, P.H., 2010. Mitochondrial and apoptotic neuronal death signaling pathways in cerebral ischemia. Biochim. Biophys. Acta 1802 (1), 92–99. http://dx.doi.org/10.1016/j.bbadis.2009.09.002.

Olichon, A., Baricault, L., Gas, N., Guillou, E., Valette, A., Belenguer, P., Lenaers, G., 2003. Loss of OPA1 perturbates the mitochondrial inner membrane structure and integrity, leading to cytochrome *c* release and apoptosis. J. Biol. Chem. 278 (10), 7743–7746. http://dx.doi.org/10.1074/jbc.C200677200.

Ong, S.B., Subrayan, S., Lim, S.Y., Yellon, D.M., Davidson, S.M., Hausenloy, D.J., 2010. Inhibiting mitochondrial fission protects the heart against ischemia/reperfusion injury. Circulation 121 (18), 2012–2022. http://dx.doi.org/10.1161/CIRCULATIONAHA.109.906610.

Owens, K., Park, J.H., Gourley, S., Jones, H., Kristian, T., 2015. Mitochondrial dynamics: cell-type and hippocampal region specific changes following global cerebral ischemia. J. Bioenerg. Biomembr. 47 (1–2), 13–31. http://dx.doi.org/10.1007/s10863-014-9575-7.

Sanderson, T.H., Wider, J.M., 2013. 2-vessel occlusion/hypotension: a rat model of global brain ischemia. J. Visual. Exp. 76. http://dx.doi.org/10.3791/50173.

Sanderson, T.H., Kumar, R., Sullivan, J.M., Krause, G.S., 2008. Insulin blocks cytochrome *c* release in the reperfused brain through PI3-K signaling and by promoting Bax/Bcl-XL binding. J. Neurochem. 106 (3), 1248–1258.

Sanderson, T.H., Mahapatra, G., Pecina, P., Ji, Q., Yu, K., Sinkler, C., Varughese, A., Kumar, R., Bukowski, M.J., Tousignant, R.N., Salomon, A.R., Lee, I., Huttemann, M., 2013. Cytochrome *c* is tyrosine 97 phosphorylated by neuroprotective insulin treatment. PLoS One 8 (11). http://dx.doi.org/10.1371/journal.pone.0078627.

Sanderson, T.H., Raghunayakula, S., Kumar, R., 2015a. Release of mitochondrial Opa1 following oxidative stress in HT22 cells. Mol. Cell. Neurosci. 64, 116–122. http://dx.doi.org/10.1016/j.mcn.2014.12.007.

Sanderson, T.H., Raghunayakula, S., Kumar, R., 2015b. Neuronal hypoxia disrupts mitochondrial fusion. Neuroscience http://dx.doi.org/10.1016/j.neuroscience.2015.05.078.

Sanderson, T.H., Raghunayakula, S., Kumar, R., 2015c. Release of mitochondrial Opa1 following oxidative stress in HT22 cells. Mol. Cell. Neurosci. 64, 116–122. http://dx.doi.org/10.1016/j.mcn.2014.12.007.

Sims, N.R., Pulsinelli, W.A., 1987. Altered mitochondrial respiration in selectively vulnerable brain subregions following transient forebrain ischemia in the rat. J. Neurochem. 49 (5), 1367–1374.

Smith, M.L., Bendek, G., Dahlgren, N., Rosen, I., Wieloch, T., Siesjo, B.K., 1984. Models for studying long-term recovery following forebrain ischemia in the rat. 2. A 2-vessel occlusion model. Acta Neurol. Scand. 69 (6), 385–401.

Sobrado, M., Ramirez, B.G., Neria, F., Lizasoain, I., Arbones, M.L., Minami, T., Redondo, J.M., Moro, M.A., Cano, E., 2012. Regulator of calcineurin 1 (Rcan1) has a protective role in brain ischemia/reperfusion injury. J. Neuroinflammation 9, 48. http://dx.doi.org/10.1186/1742-2094-9-48.

Varanita, T., Soriano, M.E., Romanello, V., Zaglia, T., Quintana-Cabrera, R., Semenzato, M., Menabo, R., Costa, V., Civiletto, G., Pesce, P., Viscomi, C., Zeviani, M., Di Lisa, F., Mongillo, M., Sandri, M., Scorrano, L., 2015. The opa1-dependent mitochondrial cristae remodeling pathway controls atrophic, apoptotic, and ischemic tissue damage. Cell Metab. 21 (6), 834–844. http://dx.doi.org/10.1016/j.cmet.2015.05.007.

Wang, J.X., Jiao, J.Q., Li, Q., Long, B., Wang, K., Liu, J.P., Li, Y.R., Li, P.F., 2011. miR-499 regulates mitochondrial dynamics by targeting calcineurin and dynamin-related protein-1. Nat. Med. 17 (1), 71–78. http://dx.doi.org/10.1038/nm.2282.

Wasiak, S., Zunino, R., McBride, H.M., 2007. Bax/Bak promote sumoylation of DRP1 and its stable association with mitochondria during apoptotic cell death. J. Cell Biol. 177 (3), 439–450. http://dx.doi.org/10.1083/jcb.200610042.

Wittig, I., Braun, H.P., Schagger, H., 2006. Blue native PAGE. Nat. Protoc. 1 (1), 418–428. http://dx.doi.org/10.1038/nprot.2006.62.

Wong, E.D., Wagner, J.A., Gorsich, S.W., McCaffery, J.M., Shaw, J.M., Nunnari, J., 2000. The dynamin-related GTPase, Mgm1p, is an intermembrane space protein required for maintenance of fusion competent mitochondria. J. Cell Biol. 151 (2), 341–352.

Yamaguchi, R., Lartigue, L., Perkins, G., Scott, R.T., Dixit, A., Kushnareva, Y., Kuwana, T., Ellisman, M.H., Newmeyer, D.D., 2008. Opa1-mediated cristae opening is Bax/Bak and BH3 dependent, required for apoptosis, and independent of Bak oligomerization. Mol. Cell 31 (4), 557–569. http://dx.doi.org/10.1016/j.molcel.2008.07.010.

Zhang, X., Yan, H., Yuan, Y., Gao, J., Shen, Z., Cheng, Y., Shen, Y., Wang, R.R., Wang, X., Hu, W.W., Wang, G., Chen, Z., 2013. Cerebral ischemia-reperfusion-induced autophagy protects against neuronal injury by mitochondrial clearance. Autophagy 9 (9), 1321–1333. http://dx.doi.org/10.4161/auto.25132.

Zuo, W., Zhang, S., Xia, C.Y., Guo, X.F., He, W.B., Chen, N.H., 2014. Mitochondria autophagy is induced after hypoxic/ischemic stress in a Drp1 dependent manner: the role of inhibition of Drp1 in ischemic brain damage. Neuropharmacology 86, 103–115. http://dx.doi.org/10.1016/j.neuropharm.2014.07.002.